

1
2 **Depolarizing GABA Transmission Restrains Activity-Dependent**
3 **Glutamatergic Synapse Formation in the Developing**
4 **Hippocampal Circuit**

5
6 Short Title: GABA Restrains Excitatory Synapse Formation

7
8 Christopher K. Salmon¹, Horia Pribiag¹, W. Todd Farmer¹, Scott Cameron¹, Emma V.
9 Jones¹, Vivek Mahadevan², David Stellwagen¹, Melanie A. Woodin²,
10 and Keith K. Murai^{1*}

11
12
13 ¹Centre for Research in Neuroscience, Department of Neurology and Neurosurgery, The
14 Research Institute of the McGill University Health Centre, Montreal General Hospital,
15 Montreal, Quebec, H3G 1A4, Canada.

16 ²Department of Cell & Systems Biology, University of Toronto, Toronto, Ontario, M5S
17 3G5, Canada.

18
19
20 *Correspondence should be addressed to:

21 Dr. Keith K. Murai
22 Centre for Research in Neuroscience
23 Montreal General Hospital
24 1650 Cedar Avenue L7-212
25 Montreal, QC, H3G 1A4 Canada
26 Telephone: (514) 934-1934 x43477
27 Fax: (514) 934-8216
28 keith.murai@mcgill.ca

29
30
31 **Number of figures:** 4

32 **Supplementary figures:** 5

33 **Number of words:** 8631 (Abstract 285; Intro 641; Discussion 1563)

34
35 **Key Words:** Synapse formation, hippocampus, GABA transmission, dendritic spines,
36 chloride homeostasis, KCC2, circuit development, autism

37
38 **Acknowledgements:** The authors would like to thank Dr. Andrew Greenhalgh and Andy
39 YL Gao for critical review of the manuscript. This work was supported by the Canadian
40 Institutes of Health Research (M.A.W and K.K.M) and Natural Sciences and Engineering
41 Research Council of Canada (K.K.M). C.K.S. was supported through a CGS-M from the
42 CIHR and a Doctoral Award from the FRQS. The authors declare no competing financial
43 interests.

44

45 **ABSTRACT**

46 GABA is the main inhibitory neurotransmitter in the mature brain but has the paradoxical
47 property of depolarizing neurons during early development. Depolarization provided by
48 GABA_A transmission during this early phase regulates neural stem cell proliferation,
49 neural migration, neurite outgrowth, synapse formation, and circuit refinement, making
50 GABA a key factor in neural circuit development. Importantly, depending on the context,
51 depolarizing GABA_A transmission can either drive neural activity, or inhibit it through
52 shunting inhibition. The varying roles of depolarizing GABA_A transmission during
53 development, and its ability to both drive and inhibit neural activity, makes it a difficult
54 developmental cue to study. This is particularly true in the later stages of development,
55 when the majority of synapses form and GABA_A transmission switches from depolarizing
56 to hyperpolarizing. Here we addressed the importance of depolarizing but inhibitory (or
57 shunting) GABA_A transmission in glutamatergic synapse formation in hippocampal CA1
58 pyramidal neurons. We first showed that the developmental depolarizing-to-
59 hyperpolarizing switch in GABA_A transmission is recapitulated in organotypic
60 hippocampal slice cultures. Based on the expression profile of K⁺-Cl⁻ co-transporter 2
61 (KCC2) and changes in the GABA reversal potential, we pinpointed the timing of the
62 switch from depolarizing to hyperpolarizing GABA_A transmission in CA1 neurons. We
63 found that blocking depolarizing but shunting GABA_A transmission increased excitatory
64 synapse number and strength, indicating that depolarizing GABA_A transmission can
65 restrain glutamatergic synapse formation. The increase in glutamatergic synapses was
66 activity-dependent, but independent of BDNF signalling. Importantly, the elevated number
67 of synapses was stable for more than a week after GABA_A inhibitors were washed out.
68 Together these findings point to the ability of immature GABAergic transmission to
69 restrain glutamatergic synapse formation and suggest an unexpected role for depolarizing
70 GABA_A transmission in shaping excitatory connectivity during neural circuit development.

71

72 **INTRODUCTION**

73 γ -Aminobutyric acid (GABA) is the main inhibitory neurotransmitter in the mature
74 brain. However, GABA is paradoxically depolarizing during nervous system development.
75 Many *in vitro* studies in rodents have shown that depolarizing GABA_A transmission

76 provides excitatory drive during gestation and early postnatal CNS development, driving
77 early network oscillations (ENOs) thought to promote activity-dependent maturation of
78 neural circuits (Ben-Ari et al., 2012). However, recent work suggests that despite
79 providing local depolarization, immature GABA_A transmission has inhibitory effects *in vivo*
80 (Kirmse et al., 2015; Oh et al., 2016; Valeeva et al., 2016). This ability of GABA to be
81 simultaneously depolarizing and inhibitory relies on shunting inhibition, which results from
82 a decrease in input resistance and membrane time constant when GABA_A receptors
83 open, regardless of the direction of Cl⁻ flux (Staley and Mody, 1992). Importantly, shunting
84 inhibition can occur in conjunction with both hyperpolarizing and depolarizing GABA_A
85 transmission, and we therefore refer to the latter case as depolarizing/inhibitory.

86 Depolarizing GABA_A transmission is implicated in numerous neurodevelopmental
87 processes in vertebrates, including neural stem cell proliferation (Liu et al., 2005), cell
88 migration (Behar et al., 2000), neurite outgrowth (Cancedda et al., 2007), synapse
89 formation, and circuit refinement (Akerman and Cline, 2006; Cancedda et al., 2007; Wang
90 and Kriegstein, 2008). Critically, circuit activity supported by depolarizing GABA_A
91 transmission *in vitro* drives calcium influx thought to be important for glutamatergic
92 synapse development (Leinekugel et al., 1995; Ben-ari et al., 1997; Griguoli and
93 Cherubini, 2017). Indeed, disrupting the depolarizing nature of GABA_A transmission by
94 interfering with chloride homeostasis alters glutamatergic synapse formation and
95 maturation (Akerman and Cline, 2006; Wang and Kriegstein, 2008). However, the effects
96 of GABA_A transmission itself on glutamatergic synapse development and the timing of
97 these effects remain poorly defined. This is partly due to the difficulty in manipulating
98 depolarizing GABA_A transmission in defined cell types and circuits with sufficient temporal
99 resolution to specifically target the period when glutamatergic synapses are forming, while
100 sparing the preceding developmental roles of GABA. Several studies have prematurely
101 hyperpolarized the reversal potential for chloride (E_{Cl}) by disrupting chloride homeostasis
102 for more than a week during perinatal development, across a timespan in which the
103 targeted neurons terminally divide, migrate, extend neurites and are incorporated into the
104 surrounding circuitry (Ge et al., 2006; Cancedda et al., 2007; Wang and Kriegstein, 2008).
105 This work suggests that disrupting E_{Cl} alters neurite and synapse maturation, however, it
106 has been noted that additional studies with higher temporal resolution are needed

107 (Akerman and Cline, 2007; Kirmse et al., 2018). Closing this gap in our understanding of
108 how GABA_A transmission and its transition from a depolarizing to a hyperpolarizing state
109 impacts glutamatergic synapse development will help solve a now classic problem in
110 developmental neurobiology, and will likely be of clinical significance as disruptions of
111 GABA_A transmission during brain development are associated with neurodevelopmental
112 disorders (El Marroun et al., 2014; He et al., 2014; Tyzio et al., 2014).

113 Here we investigated the role of depolarizing GABA_A transmission in glutamatergic
114 synapse formation on hippocampal CA1 pyramidal cells. To perform temporally precise
115 pharmacological manipulations of GABA_A transmission during neural circuit development,
116 we took advantage of the properties of the organotypic hippocampal slice culture. This
117 preparation preserves the anatomy and the developmental progression of the
118 hippocampus, including the time course of excitatory synapse formation (Buchs et al.,
119 1993; Muller et al., 1993; De Simoni et al., 2003). This system enabled us to define a
120 narrow time window during the first week of slice development in which GABA_A
121 transmission shifts from immature, depolarizing transmission, to hyperpolarizing
122 transmission in CA1 pyramidal cells. Previous work suggests that blocking depolarizing
123 GABA_A transmission during development will remove excitatory drive and decrease
124 excitatory synapse formation and maturation (Ben-Ari et al., 2007; Wang and Kriegstein,
125 2008). Contrary to these predictions, we found that transient blockade of immature,
126 depolarizing GABA_A transmission increased glutamatergic synapse number and function
127 on CA1 pyramidal cells. This unexpected effect was explained by the finding that, at this
128 stage of development, depolarizing GABA_A transmission provides shunting inhibition,
129 which when blocked alleviated a restraint on activity-dependent synapse formation.
130 Interestingly, the activity-dependent increase in glutamatergic synapses was stable for at
131 least a week. Furthermore, the effect could not be reproduced by prematurely
132 hyperpolarizing E_{GABA}, and was independent of BDNF signalling. Our results therefore
133 point to an important time window during hippocampal development when immature
134 GABA_A transmission can restrain excitatory synapse development, and that interfering
135 with GABA_A transmission at this stage can have lasting effects on neural circuitry.

136

137 RESULTS

138 **GABA_A transmission switches from depolarizing to hyperpolarizing in CA1 cells** 139 **during the first week in hippocampal slice culture.**

140 Depolarizing GABA_A transmission relies on relatively high intracellular chloride ($[Cl^-]_i$). As
141 neurons mature during the first weeks of postnatal CNS development, Na⁺-K⁺-Cl⁻
142 cotransporter (NKCC1) expression is downregulated and K⁺-Cl⁻ cotransporter 2 (KCC2)
143 is upregulated, lowering $[Cl^-]_i$ (Rivera et al., 1999; Yamada et al., 2004). GABA_A receptors
144 are largely permeable to Cl⁻, and to a lesser extent bicarbonate (HCO₃⁻) (Kaila, 1994;
145 Staley and Proctor, 1999). When $[Cl^-]_i$ lowers to the point at which the reversal potential
146 for GABA (E_{GABA}) hyperpolarizes below the resting membrane potential, GABA_A
147 transmission switches from depolarizing to hyperpolarizing. To pinpoint when this switch
148 from depolarization to hyperpolarization occurs in CA1 pyramidal cells in hippocampal
149 organotypic slices, we first assessed the timing of KCC2 upregulation across the first two
150 weeks *in vitro* and found expression of both KCC2 monomers (KCC2-M) and oligomers
151 (KCC2-O) underwent a large and graded increase between 3 and 7DIV (Fig 1A,B),
152 reaching near-maximal levels by 7 days *in vitro* (DIV) (Fig 1B). Using this timeframe as a
153 guide, we performed gramicidin perforated patch recordings to determine the GABA_A
154 reversal potential (E_{GABA}) in CA1 pyramidal cells (exemplary traces and IV curves shown
155 in Figures 1C and D). At 3-4 DIV, E_{GABA} was depolarized with respect to resting membrane
156 potential (RMP) (Fig 1E-G). However, by 6-7 DIV E_{GABA} was hyperpolarized with respect
157 to RMP, indicating a switch to hyperpolarizing GABA_A transmission by 6-7 DIV (Fig 1C-
158 G), a timeframe similar to that reported previously for CA1 pyramidal cells (Swann et al.,
159 1989). E_{GABA} was more negative than action potential threshold at 3-4 DIV (Fig 1E,G),
160 suggesting GABA is depolarizing but not capable of directly depolarizing neurons past
161 action potential (AP) threshold from rest at this stage.

162 **Blocking depolarizing GABA_A transmission increases CA1 spine density.**

163 Overexciting mature neurons by blocking hyperpolarizing GABA_A transmission is
164 known to cause a collapse of dendritic spines both *in vivo* (Zeng et al., 2007) and *in vitro*
165 (Muller et al., 1993; Drakew et al., 1996; Jourdain et al., 2002; Zha et al., 2005). In
166 particular, applying GABA_A antagonists to organotypic hippocampal cultures at 5 or 23
167 DIV over a period of 2 to 3 days was shown to cause a robust loss of spines (Drakew et

168 al., 1996; Zha et al., 2005). Consistent with this, when we blocked GABA_A transmission
169 with the GABA_AR antagonist, bicuculline (BIC) from 5-7 DIV (when GABA_A transmission
170 is hyperpolarizing (Fig 1C-H)), spine density decreased by 34% (Fig 2A-C). This suggests
171 that by this stage, excitatory transmission causes overexcitation and spine loss in the
172 absence of hyperpolarizing GABA_A transmission.

173 To assess the role of immature, depolarizing GABA_A transmission on dendritic
174 spine development, we inhibited GABA_A transmission earlier, from 3-5 DIV (Fig 2D).
175 Previous work suggests that inhibiting depolarizing GABA_A transmission during
176 development would decrease glutamatergic synapse formation and maturation (Ben-ari
177 et al., 1997; Hanse et al., 1997; Cancedda et al., 2007; Wang and Kriegstein, 2008).
178 However, in contrast to these findings, BIC applied for 48 hours from 3 to 5 DIV
179 significantly increased dendritic spine density (25% increase)(Fig 2E-F). This effect was
180 fully reproducible with the GABA_AR antagonist gabazine (GBZ)(31% increase)(Fig 2E,G),
181 which is a more specific antagonist of GABA_ARs (Heaulme et al., 1986) and blocks
182 inhibition more consistently in hippocampal neurons (Sokal et al., 2000). We also verified
183 that the presence of penicillin-streptomycin in the culture medium was not associated with
184 this effect by blocking GABA transmission in the absence antibiotics, and found the same
185 increase in dendritic spines (S1A-C Fig).

186 To assess whether the supernumerary spines induced by blocking depolarizing
187 GABA_A transmission showed structural differences, we analyzed spine morphology. GBZ
188 treatment did not affect the proportions of mushroom, thin, and stubby spines (Fig 2H),
189 2-dimensional head area (Control: $0.32 \pm 0.02 \mu\text{m}^2$; GBZ: $0.37 \pm 0.04 \mu\text{m}^2$, $p > 0.10$), head
190 diameter (Control: $0.58 \pm 0.02 \mu\text{m}^2$; GBZ: $0.62 \pm 0.03 \mu\text{m}^2$, $p > 0.1$), spine length (Control
191 $1.66 \pm 0.09 \mu\text{m}^2$; GBZ: $1.83 \pm 0.08 \mu\text{m}^2$, $p > 0.1$) or dendrite diameter (Fig 2I).

192 We next asked whether the increased number of spines constituted an increase in
193 *bona fide* glutamatergic synapses on CA1 cells by recording miniature EPSCs (mEPSC).
194 Consistent with the increase in dendritic spine density, mEPSC analysis showed that GBZ
195 treatment (3-5 DIV) increased mEPSC frequency 3-fold (Fig 2J,K). Miniature EPSC
196 amplitude also increased, indicating enhanced synaptic strength (Fig 2L-M). Together,
197 these results suggest that immature GABA_A transmission restrains glutamatergic
198 synapse formation and maturation.

199 The narrow time window we examined raised the possibility that the spine-
200 enhancing effect of GABA_A blockade is limited to a short period directly prior to the
201 depolarizing to hyperpolarizing shift in GABA_A transmission. This would suggest that
202 GABA_A transmission restrains glutamatergic synapse formation only during a very short
203 transition state. To test whether this was the case, we prepared slices 3 days earlier (P2)
204 and applied GBZ at 3DIV for 48h (S1D Fig). We found that GABA_AR blockade in these
205 younger slices also caused a significant increase in spines (S1E,F Fig), suggesting that
206 depolarizing GABA_A transmission is capable of restraining synapse formation for an
207 appreciable period during postnatal development.

208 **Bumetanide treatment has no effect on spine numbers.**

209 Previous work suggests that abrogating GABAergic depolarization by prematurely
210 rendering GABA hyperpolarizing decreases glutamatergic synapse formation (Ge et al.,
211 2006; Wang and Kriegstein, 2008). However, our data show that a complete loss of
212 depolarizing GABA_A transmission increases glutamatergic synapse formation. These
213 contrasting results raise the question of whether the depolarizing nature of GABA_A
214 transmission is important for the normal development of glutamatergic synapse number
215 in our period of interest (3-5 DIV). To address this, we asked whether prematurely
216 hyperpolarizing E_{GABA} could mimic the effect of GABA_A blockade by treating slices with
217 the NKCC1 blocker bumetanide (BUME) from 3 to 5DIV (S2 Fig). BUME is well
218 established to lower E_{GABA} in immature neurons (Dzhala et al., 2005) and prematurely
219 render GABA hyperpolarizing (Wang and Kriegstein, 2011). Treating slice cultures at
220 3DIV with BUME did not alter spine density on its own (S2A,B Fig), indicating that the
221 depolarizing nature of GABA is not important for regulating spine numbers at this stage
222 of development. Furthermore, BUME did not alter the effect of GBZ on spine density,
223 indicating that the extent to which E_{GABA} is depolarized is not important for limiting spine
224 density to normal levels at this stage.

225 Since KCC2 overexpression can cause an increase in spines through its non-
226 transport, scaffolding function (Li et al., 2007; Fiumelli et al., 2012), we also assessed
227 KCC2 expression following GBZ treatment. GBZ did not significantly elevate expression
228 of KCC2 oligomers or monomers (S2C-E Fig).

229 **Driving depolarizing GABA_A transmission does not alter glutamatergic synapse**
230 **number.**

231 Next, we investigated if increasing GABA_A transmission over the 3-5 DIV period
232 would have the opposite effect to GABA-blockade and reduce excitatory synapses.
233 Previous work has demonstrated that propofol, a positive allosteric modulator of
234 GABA_ARs, decreases spine density in developing layer 2/3 principal cells of the
235 somatosensory cortex when administered to rat pups over a 6h period at postnatal day
236 10, when GABA_A transmission is still depolarizing (Puskarjov et al., 2017). To test this in
237 CA1 pyramidal cells, we increased depolarizing GABA_A transmission by administering
238 muscimol (MUS) or diazepam (DZP) from 3 to 5DIV. MUS treatment did not significantly
239 decrease spine density (S3A-C Fig). Furthermore, mEPSC frequency was unchanged,
240 confirming MUS did not alter synapse numbers (S3D,E Fig). MUS has varying effects on
241 different GABA receptors and can cause GABA_A receptor desensitization, making its
242 effects difficult to interpret (Heck et al., 2007; Mortensen et al., 2010; Johnston, 2014).
243 We therefore also tested whether enhancing GABA_A transmission with DZP could
244 decrease glutamatergic synapses, but this also had no effect on spine density or mEPSCs
245 (S3A-F Fig). Based on these results, increasing GABA_A transmission was not sufficient
246 to decrease glutamatergic synapse number or function, suggesting depolarizing GABA_A
247 transmission can only limit synapse formation up to a certain point at this stage of
248 development. However, our results do not rule out the possibility that enhancing immature
249 GABA_A transmission on different timescales or in other systems decreases glutamatergic
250 synapse formation (Puskarjov et al., 2017).

251 **Increased glutamatergic synapses following blockade of depolarizing GABA_A**
252 **transmission is activity-dependent.**

253 Based on our recordings showing that at 3-4DIV E_{GABA} is depolarized relative to
254 RMP, but lower than action potential threshold (Fig 1E-G), GABA is likely to mediate
255 shunting inhibition (ie depolarizing/inhibitory transmission), at this stage (see S4A Fig for
256 schematic). To test this possibility, we puffed GABA locally while recording spontaneous
257 or electrically evoked firing. GABA inhibited both spontaneous (Fig 3A,B) and evoked
258 spiking (S1B,C Fig), suggesting that although E_{GABA} is depolarizing relative to RMP,

259 GABA_A transmission is inhibitory during the 3-5 DIV timeframe. Blocking this
260 depolarizing/inhibitory GABA_A transmission likely increased activity in our preparation,
261 suggesting that the increase in glutamatergic synapses following GABA-blockade at 3DIV
262 may be driven by activity-dependent mechanisms (Balkowiec and Katz, 2002; Pérez-
263 Gómez and Tasker, 2013). To address this hypothesis, we measured levels of *Bdnf* and
264 *Fos* mRNA, two activity regulated genes associated with glutamatergic synapse formation
265 (Vicario-Abejón et al., 1998, 2002; Tyler and Pozzo-Miller, 2003; Chapleau et al., 2009).
266 Both transcripts were significantly upregulated following 48-hour blockade of
267 depolarizing/inhibitory GABA_A transmission (*Bdnf*: 5-fold increase, *Fos*: 2.5-fold increase)
268 (Fig 3C). GABA_A blockade at 3DIV also increased Fos protein expression after 24 and 48
269 hours (Fig 3D-E). Together these data indicate that blocking immature depolarizing
270 GABA_A transmission at this point caused an increase in activity in CA1 pyramidal cells.
271 To test whether the increased synapse formation we observed following GABA blockade
272 at 3DIV was activity-dependent, we treated slice cultures with GBZ and/or TTX, and found
273 that while TTX alone had no effect on spine density, TTX blocked the GBZ-induced
274 increase in spines (Fig 3F). From this we conclude that depolarizing/inhibitory GABA_A
275 limits activity-dependent glutamatergic synapse formation at this point in the development
276 of hippocampal circuitry in slice culture.

277 BDNF is known to regulate activity-dependent synapse formation and plasticity
278 (Park and Poo, 2013), and we therefore asked whether BDNF signaling was responsible
279 for the increase in spines following blockade of depolarizing/inhibitory GABA_A
280 transmission. We inhibited BDNF signalling during the 3 to 5DIV GBZ treatment using
281 TrkB-Fc bodies or K252a (Ji et al., 2010; Puskarjov et al., 2014), however neither
282 approach blocked the increase in spine density (Fig 3G,H), suggesting that BDNF
283 signalling is not necessary for the observed increase in spines.

284 **Blocking depolarizing GABA_A transmission leads to a sustained increase in** 285 **glutamatergic synapses.**

286 The observed increase in spine density induced by blocking depolarizing/inhibitory
287 GABA_A transmission may only lead to a transient alteration without a longer lasting effect
288 on glutamatergic synapses. To determine whether blockade of GABA_A transmission
289 caused a temporary or sustained increase in glutamatergic synapses, we treated slices

290 with GBZ from 3-5 DIV and allowed them to recover for an additional 5-9 days in the
291 absence of GBZ (Fig 4A). This temporary GABA_A blockade resulted in a 37% increase in
292 spine density after a 5-day recovery period (Fig 4B,C). Furthermore, after this recovery
293 period, CA1 cells had more thin spines than mushroom spines, a difference not present
294 in the control condition (Fig 4D). No changes in dendrite diameter were observed (Fig
295 4E). To determine if transient GBZ treatment led to long-term functional changes in
296 glutamatergic synapses, we recorded mEPSC frequency and amplitude after 8-9 days of
297 recovery. We found that mEPSC frequency was enhanced by 79%, while mEPSC
298 amplitude was unchanged at this stage (Fig 4F-I). Together these data suggest that
299 inhibiting depolarizing GABA_A transmission during a narrow time window can lead to
300 persistent changes in glutamatergic synapse number in the hippocampus.

301 **DISCUSSION**

302 Immature, depolarizing GABA_A transmission is believed to promote glutamatergic
303 synapse formation and maturation (Ben-ari et al., 1997; Hanse et al., 1997; Wang and
304 Kriegstein, 2009; Chancey et al., 2013). However, when and how GABA affects
305 glutamatergic synapse formation remains to be fully understood. Indeed, several groups
306 have noted that tools and approaches for manipulating depolarizing GABA_A transmission
307 with higher temporal and spatial precision are needed to resolve this (Akerman and Cline,
308 2007; Chancey et al., 2013; Kirmse et al., 2018). We therefore sought to address the role
309 of GABA_A transmission in glutamatergic synapse formation by performing precisely timed
310 pharmacological manipulations in hippocampal slice cultures. We first mapped the
311 depolarizing-to-hyperpolarizing shift of GABA_A transmission in CA1 cells. This was
312 followed by structural and electrophysiological analysis which showed that blocking
313 immature, depolarizing/inhibitory GABA_A transmission enhanced glutamatergic synapse
314 function and number. Interestingly, the enhanced synapse number was stable following
315 a recovery period. These results suggest that immature GABA_A transmission restrains
316 glutamatergic synapse formation during an early phase of hippocampal circuit
317 development. Using slice cultures allowed for more temporally precise manipulations that
318 revealed this effect, though limitations of this model system must be considered when
319 interpreting our results. In particular, exuberant glutamatergic synapse formation has

320 been observed in slice cultures, and has been attributed to increases in distal dendritic
321 branching (De Simoni et al., 2003). However, we minimized this confound by focusing on
322 primary apical dendrites, which are fully formed by the time of pharmacological treatment.
323 Thus, while further work will be required to extend our findings to other systems, the
324 results of this study show that immature, depolarizing GABA_A transmission is capable of
325 restraining glutamatergic synapse formation in certain contexts, and that the removal of
326 this restraint by interfering with GABA_A transmission during development may cause a
327 long-term increase in glutamatergic synapses.

328 **An unpredicted role for immature GABA_A transmission in restraining glutamatergic** 329 **synapse formation**

330 In the time window we examined, GABA_A transmission provides subthreshold
331 depolarization and shunting inhibition, which when blocked alleviates a brake on
332 glutamatergic synapse development. Taken in the context of previous work, our results
333 suggest a couple of models for how immature GABA_A transmission affects hippocampal
334 excitatory connectivity (S5 Fig). Firstly, the GABA-mediated restraint on glutamatergic
335 synapse formation may be a short-lived feature of a depolarizing/inhibitory transition state
336 that GABA passes through as E_{Cl} matures from depolarizing and excitatory to
337 hyperpolarizing (Model 1, S5A-C Fig). However, recent work suggests GABA may be
338 inhibitory throughout most or all of postnatal development. Therefore, in a second model,
339 depolarizing but inhibitory GABA_A transmission may inhibit circuit activity from birth
340 onward (Model 2, S5B-C Fig), thus restraining glutamatergic synapse formation across
341 development.

342 The first model is based on evidence from acute slices suggesting that immature
343 GABA_A transmission is capable of driving excitation (Gulledge and Stuart, 2003) and that
344 depolarizing GABA_A transmission drives ENOs, which in turn promote glutamatergic
345 synapse formation and unsilencing, and circuit refinement (Hanse et al., 1997; Ben-Ari,
346 2002; Wang and Kriegstein, 2009; Griguoli and Cherubini, 2017). Disrupting E_{Cl} or GABA_A
347 transmission in this phase of development is hypothesized to interfere with synapse
348 formation (S5A Fig), and this has been borne out by experimentally lowering E_{Cl} across
349 the postmitotic period in immature neurons (Ge et al., 2006; Cancedda et al., 2007; Wang

350 and Kriegstein, 2008). Incorporating our results refines this model and accounts for the
351 role of GABA_A transmission in circuit development as it transitions from a depolarizing
352 and excitatory to a hyperpolarizing state. Our work suggests that following an initial
353 depolarizing phase in which GABA promotes excitation, as E_{Cl} progressively matures,
354 GABA_A transmission passes through a transient but developmentally relevant
355 depolarizing/inhibitory phase (S5B Fig). Such a transition phase is hinted at in the
356 literature, as certain studies have shown that blocking depolarizing GABA_A transmission
357 can silence ENOs, while others show GABA_A blockade to increase circuit activity by
358 eliciting interictal discharges or paroxysmal activity (Le Magueresse et al., 2006; Ben-Ari
359 et al., 2007). Our results suggest that during this transition phase, depolarizing GABA_A
360 transmission is inhibitory and restrains glutamatergic synapse formation. Blocking GABA_A
361 transmission at this time alleviates the restraint, allowing for activity-dependent synapse
362 formation (S5B Fig). Following this transition phase, GABA_A transmission becomes fully
363 hyperpolarizing as the glutamatergic system becomes capable of overexcitation. The
364 result of GABA_A blockade at this stage is loss of spines (Fig 2 and S5C Fig) (Swann et
365 al., 1989; Drakew et al., 1996; Zeng et al., 2007). Interestingly, the absence of a similar
366 spine loss following blockade of depolarizing/inhibitory GABA_A transmission at 3DIV
367 suggests that, while this still immature GABAergic inhibition is important for regulating
368 activity levels, the glutamatergic system is not yet mature enough to cause a pathological
369 collapse of synapse numbers similar to that seen in models of epilepsy (29,30).

370 Alternatively, in a second model, it is possible that depolarizing GABA_A
371 transmission provides shunting inhibition throughout the postnatal period, thereby
372 restraining synapse formation and circuit activity during development (S5B-C Fig, green
373 shaded area). Indeed, emerging evidence suggests that depolarizing GABA_A
374 transmission exerts inhibitory effects on ENOs *in vivo*, from at least P3 onward (Kirmse
375 et al., 2015; Valeeva et al., 2016; Che et al., 2018). Consistent with this, our results in
376 slices cultured from younger mice (S1D-F Fig) suggest that GABA_A transmission restrains
377 synapse formation over a period of up to 5 days of hippocampal circuit development.
378 While previous work has admittedly demonstrated that prematurely rendering GABA_A
379 transmission hyperpolarizing *in vivo* decreases glutamatergic synapse formation (Ge et
380 al., 2006; Cancedda et al., 2007; Wang and Kriegstein, 2008, 2011), it is noteworthy that

381 these earlier studies manipulated E_{Cl} over extended periods that spanned multiple phases
382 of postmitotic neuronal development, including cell migration, axonal/dendritic growth,
383 synapse formation and circuit refinement. Depolarizing GABA_A transmission is thought to
384 play important roles in all of these processes (Owens and Kriegstein, 2002), and hence
385 the observed effects of prematurely reducing E_{Cl} on synapses may be secondary to other
386 alterations in neuronal and circuit development. Indeed, soma size and dendritic
387 branching are altered when GABA is prematurely rendered hyperpolarizing over an
388 extended time period (Cancedda et al., 2007; Wang and Kriegstein, 2008). More
389 temporally precise manipulations of GABA_A transmission and E_{Cl} are therefore essential
390 for clarifying the roles of GABA during critical phases of synapse formation *in vivo*.
391 Interestingly, the finding that propofol administered to postnatal day 10 rats decreased
392 spine number supports the notion that there is a developmental period *in vivo* during
393 which immature GABA_A transmission restrains glutamatergic synapse formation
394 (Puskarjov et al., 2017).

395 When considering these two models, it is important to note that an inhibitory effect
396 of depolarizing GABA_A transmission does not preclude a role for GABA in driving ENOs,
397 as it has been demonstrated that depolarizing chloride currents are only involved in the
398 initial generation of GDPs in acute slices, after which they inhibit the continuation of the
399 same GDPs (Khalilov et al., 2015). Thus, depolarizing GABA_A transmission may
400 simultaneously generate ENOs, while also maintaining control of wider circuit activity,
401 thereby limiting runaway glutamatergic synapse formation. These dichotomous effects of
402 GABA may rely on where GABAergic inputs impinge on the post synaptic neuron.
403 Gullledge and Steward (2003) showed that in young rats, puffing GABA on distal dendrites
404 of Layer 5 pyramidal cells facilitated firing, while puffing GABA on the cell body inhibited
405 firing. Thus, different GABAergic interneuron subtypes may be responsible for driving
406 ENOs vs restraining glutamatergic synapse formation. Furthermore, despite the evidence
407 suggesting GABA is inhibitory throughout most of postnatal development *in vivo*, it has
408 been shown that high frequency uncaging or stimulated release of GABA onto dendrites
409 of layer 2/3 pyramidal cells in the neocortex can elicit formation of glutamatergic and
410 GABAergic synapses during development *in vivo* (Oh et al., 2016). Although it remains to
411 be seen whether endogenous patterns of GABA release can have similar effects, it

412 appears there may be a local trophic role for depolarizing GABA_A transmission, which
413 may promote synapse formation even as its circuit-wide inhibitory effects restrain the
414 same process as we have demonstrated. More work is needed to dissect the possible
415 roles of GABA in local synapse formation and more global circuit development, and to
416 understand how the role of GABA changes across development.

417 **Sustained Changes in Glutamatergic Synapses and Neurodevelopmental** 418 **Disorders**

419 Remarkably, we found that a transient blockade of depolarizing, inhibitory GABA_A
420 transmission led to a sustained increase in both the number of glutamatergic synapses
421 and the proportion of thin spines, indicating that transient manipulations of immature
422 GABA_A transmission can profoundly alter hippocampal connectivity (Fig 4). Using slice
423 cultures allowed for more temporally precise manipulations that revealed this effect,
424 though it remains to be seen if the phenomenon persists *in vivo*. These questions are
425 clinically relevant, as a role for GABA in restraining synapse formation may change how
426 we understand and mitigate the effects of anticonvulsants, anaesthetics and drugs of
427 abuse on neonatal, as well as fetal development, as GABA is believed to be depolarizing
428 mainly in late gestation in humans (Vanhatalo et al., 2005; Sedmak et al., 2015).
429 Furthermore, both the persistent increase in synapses and spines and the shift in spine
430 morphologies we observed after recovery from transient GBZ treatment are reminiscent
431 of “spinopathies” seen in intellectual disabilities including Fragile X syndrome and autism
432 spectrum disorders (Lacey and Terplan, 1987; Irwin et al., 2000, 2001; Kaufmann and
433 Moser, 2000; Fiala et al., 2002; Hutsler and Zhang, 2010). Numerous models of ASDs
434 are associated with a delay in the depolarizing to hyperpolarizing shift in E_{GABA} (He et al.,
435 2014; Tyzio et al., 2014; Leonzino et al., 2016). Such a delayed transition to
436 hyperpolarizing E_{GABA} likely translates to a delay in the onset of adequate shunting
437 inhibition when GABA is still depolarizing, which may increase glutamatergic synapse
438 formation in a manner similar to that which we observed when blocking
439 depolarizing/inhibitory GABA_A transmission. Furthermore, mutation of the $\beta 3$ GABA_A
440 receptor subunit, the expression of which peaks during development when GABA is
441 depolarizing, has been observed in ASD (Menold et al., 2001; Buxbaum et al., 2002; Chen
442 et al., 2014). The findings presented in the current study may provide a causal link

443 between these mutations and the hyperconnectivity observed in ASDs. Thus, further
444 investigation is required to understand if impairments of depolarizing/inhibitory GABA_A
445 transmission contribute to the lasting alterations of spines and synapses in these
446 conditions. Finally, the possibility that GABA bidirectionally controls synapse formation
447 may yield novel clinical approaches for correcting synaptic deficits in neurodevelopmental
448 disorders.

449

450

451 **MATERIALS AND METHODS**

452 *Animals*

453 Experiments were approved by the Montreal General Hospital Facility Animal Care
454 Committee and followed guidelines of the Canadian Council on Animal Care. Male and
455 female C57BL6 mice kept on a 12:12 light-dark cycle were used to prepare organotypic
456 cultures.

457 *Slice Preparation*

458 Organotypic hippocampal slices were prepared as described previously (Haber et al.,
459 2006). Briefly, hippocampi were extracted from postnatal day 5 mice and cut into 300µm
460 slices with a McIlwain tissue chopper (Stoelting). Slices were cultured on semiporous
461 tissue culture inserts (Millipore) that sat in culture medium composed of minimal essential
462 medium (MEM) supplemented with Glutamax (Invitrogen, Cat. No. 42360032), 25% horse
463 serum (Invitrogen, Cat. No. 26050088), 25% HBSS (Invitrogen, Cat. No. 14025092), 6.5
464 mg/mL D-glucose and 0.5% penicillin/streptomycin. Slices were cultured for 5-14 days
465 with full medium changes every 2 days.

466 *Labeling of CA1 Cells*

467 Dendrites and spines of CA1 pyramidal cells were labelled using a Semliki Forest Virus
468 (SFV)-mediated approach describe in detail elsewhere (Haber et al., 2006). Briefly, SFV
469 driving expression of enhanced green fluorescent protein, targeted to the cell membrane
470 through a farnesylation sequence (EGFPf), was injected into the stratum oriens via pulled
471 glass pipette, broken to a diameter of approximately 50 to 100 µm. Glass pipettes were
472 attached to a Picospritzer III (Parker Hannifin) and SFV was delivered with 10ms pulses

473 at 14 to 18 psi 18 to 20 hours before fixation in 4% formaldehyde/0.1 M PO_4^{2-} for 30 min.

474 *Confocal Imaging and Spine Analysis*

475 Imaging was performed using an Ultraview Spinning Disc confocal system (Perkin Elmer)
476 attached to a Nikon TE-2000 microscope and a FV1000 laser scanning confocal
477 microscope (Olympus). Z-stacks were acquired from approximately 100 μm of CA1
478 primary apical dendrites, just above the primary dendrite bifurcation. This dendritic
479 subfield is consistently identifiable, fully formed by the period of interest, harbors the
480 highest density of asymmetric synapses, and retains its native connectivity in organotypic
481 slices (Megias et al., 2001; Amaral and Lavenex, 2007). Ten to forty z-stacks were
482 acquired per animal (2-4 animals per experiment, minimum 3 experiments per dataset).
483 Two-dimensional spine counts and geometric measurements of spines were quantified
484 using Reconstruct (Fiala, 2005) and a custom ImageJ macro. 3D spine classification was
485 performed with NeuronStudio (Rodriguez et al., 2008). All spine analysis was performed
486 by an investigator blinded to the experimental condition.

487 *Western Blot Analysis*

488 For Western blots, 4-6 organotypic slices were lifted from nylon culture inserts with a No.
489 10 scalpel blade, rinsed in cold PBS and incubated on ice in 100 μL of Triton lysis buffer
490 (20 mM Tris pH7.4, 137 mM NaCl, 2mM EDTA, 1% Triton X-100 (TX-100), 0.1% SDS,
491 10% glycerol, with protease inhibitors and sodium orthovanadate) for 30 min. Lysates
492 were centrifuged at high speed for 10 min and stored at -80°C in sample buffer.
493 Supernatants were warmed to room temperature and run under standard SDS-PAGE
494 conditions. Membranes were immunoblotted with anti-KCC2 1:1000 (N1/12, NeuroMab,
495 CA) and GAPDH 1:300,000 (MAB374, Millipore). KCC2 blots were run immediately after
496 developmental time courses ended to reduce experimentally-induced aggregation of
497 KCC2 oligomers, which we observe to increase with time at -80°C .

498 *Electrophysiology*

499 Gramicidin perforated patch whole cell recordings were performed similar to previously
500 described (Acton et al., 2012). Briefly, current-voltage (IV) curves were generated by step
501 depolarizing the membrane potential in 10mV increments from ~ -95 to -35mV (Fig 1C)
502 and during each increment GABAergic transmission was elicited via extracellular

503 stimulation in the stratum radiatum. Pipettes had a resistance of 7–12 M Ω and were filled
504 with an internal solution containing 150mM KCl, 10mM HEPES, and 50mM μ g/ml
505 gramicidin (pH 7.4, 300 mOsm). We recorded E_{GABA} in current clamp mode.
506 Glutamatergic transmission was inhibited with CNQX.

507 Miniature EPSCs (mEPSCs) were recorded using the whole-cell patch clamp
508 configuration ($V_h = -70$ mV), at 30°C, in ACSF containing (in mM): 119 NaCl, 26.2
509 NaHCO₃, 11 D-glucose, 2.5 KCl, 1 NaH₂PO₄, 2.5 CaCl₂, 1.3 MgCl₂, 0.0002 TTX, 0.025
510 D-APV, 0.05 picrotoxin. Recording pipettes (2-5 M Ω) were filled with (in mM): 122
511 CsMeSO₄, 8 NaCl, 10 D-glucose, 1 CaCl₂, 10 EGTA, 10 HEPES, 0.3 Na₃GTP, 2 MgATP,
512 pH 7.2. Signals were low-pass filtered at 2kHz, acquired at 10 kHz, and analyzed using
513 Clampfit 10.3 (Molecular Devices).

514 For cell attached recordings, ACSF and pipette solutions were as described above for
515 mEPSC recordings, but ACSF lacked TTX, D-APV and picrotoxin. Low resistance
516 recording pipettes (1-2 M Ω) were used to form loose patch seals (approximately 100-350
517 M Ω). Recordings were performed in I=0 mode. GABA was diluted in ACSF to 100 μ M and
518 puffed in close proximity to the recorded cell using a glass pipette connected to a
519 Picospritzer III (Parker Hannifin) delivering 10 ms duration air puffs at 14 psi. Electrically-
520 evoked stimulations (1.3 V, 0.5 ms) were delivered by the recording amplifier via the
521 recording pipette. Recorded signals were analyzed using threshold-based detection of
522 spikes in Clampfit 10.3 (Molecular Devices).

523 Experiments comprised slices from at least 3 separate animals taken from at least 2
524 litters.

525 *Pharmacology*

526 Pharmacological agents (Tocris unless otherwise noted) were applied to the culture
527 medium during a regular medium change. Gabazine (GBZ) (20 μ M), bicuculline-
528 methiodide (20 μ M) and muscimol (10 μ M) were used to manipulate GABA_A transmission.
529 GBZ was washed out by incubating slices in fresh medium for 30 minutes, then washing
530 the top of the slices with equilibrated medium for 1-2 minutes before changing to fresh
531 dishes and medium. Bumetanide (Bume, 10 μ M), TrkB-Fc bodies (5mg/mL, R&D
532 Systems) and K252a (200 nM) were added to cultures 30 minutes before adding GBZ.

533 *Quantitative Reverse Transcriptase PCR (qRT-PCR)*

534 Six to eight organotypic slices per sample were lifted from nylon culture inserts with a No.
535 10 scalpel blade, washed briefly in ice cold PBS and flash frozen in microcentrifuge tubes
536 in a 100% EtOH/dry ice slurry. Total RNA was extracted using the RNeasy Lipid Tissue
537 Kit (Qiagen). cDNA libraries were created using QuantiTect Reverse Transcription Kit
538 (Qiagen). Quantitative PCR was performed using Sybr Green Master Mix (Applied
539 Biosystems Systems) on a StepOne Plus thermocycler (Applied Biosystems). Relative
540 levels of mRNA were calculated using the $\Delta\Delta CT$ method with GAPDH as the internal
541 control. Primer sequences were as follows: GAPDH forward TTG AAG TCG CAG GAG
542 ACA ACC; GAPDH reverse ATG TGT CCG TCG TGG ATC; BDNF forward GTG ACA
543 GTA TTA GCG AGT GGG; BDNF reverse GGG ATT ACA CTT GGT CTC GTA G; Fos
544 forward TCC CCA AAC TTC GAC CAT G; Fos reverse CAT GCT GGA GAA GGA GTC
545 G.

546 *Immunofluorescence*

547 Slice cultures were fixed as described above, permeabilized for 30 minutes in 1% TritonX
548 100/PBS, blocked in 10% normal donkey serum (NDS, Jackson Immuno Research)/ 0.2%
549 TX-100/PBS, and incubated with anti-c-Fos antibody (1:5000, Cat. No. 226 003, Synaptic
550 Systems) in 1% NDS/0.2% TX-100/PBS rocking at 4°C for 5 days. Primary antibody
551 solution was washed with 3 rinses in 1% NDS/0.2% TX-100/PBS, followed by secondary
552 antibodies at 1:1000 for 2 hours at room temp. TOPRO-3-iodide (Jackson Immuno
553 Research) was applied at 1:10,000 for 10 minutes in the second of three washes following
554 incubation with secondary antibodies. Quantification of fluorescence intensity with
555 background correction was performed with ImageJ, using mean pixel values in ROIs
556 traced manually around cell bodies.

557 *Statistics*

558 Data is presented as mean \pm SEM. Student t-tests were used except where noted that
559 Mann-Whitney tests were used with datasets with non-normal distribution. Post hoc
560 pairwise comparisons following ANOVA were performed with Tukey's honestly significant

561 difference (HSD) test. For mean comparisons: * $p < 0.05$, ** $p < 0.01$, *** $p < 0.001$. For
562 Kolmogorov-Smirnov tests: *** $p < 0.0001$.

563

564

565

566

567

568 **REFERENCES**

- 569 Acton BA, Mahadevan V, Mercado A, Uvarov P, Ding Y, Pressey J, Airaksinen MS,
570 Mount DB, Woodin MA (2012) Hyperpolarizing GABAergic transmission requires
571 the KCC2 C-terminal ISO domain. *J Neurosci* 32:8746–8751.
- 572 Akerman CJ, Cline HT (2006) Depolarizing GABAergic conductances regulate the
573 balance of excitation to inhibition in the developing retinotectal circuit in vivo. *J*
574 *Neurosci* 26:5117–5130.
- 575 Akerman CJ, Cline HT (2007) Refining the roles of GABAergic signaling during neural
576 circuit formation. *Trends Neurosci* 30:382–389.
- 577 Amaral D, Lavenex P (2007) *The Hippocampus Book* (Andersen P, Morris R, Amaral D,
578 Bliss T, O’Keefe J, eds). Oxford: Oxford University Press.
- 579 Balkowiec A, Katz DM (2002) Cellular mechanisms regulating activity-dependent
580 release of native brain-derived neurotrophic factor from hippocampal neurons. *J*
581 *Neurosci* 22:10399–10407.
- 582 Behar TN, Schaffner AE, Scott CA, Greene CL, Barker JL (2000) GABA receptor
583 antagonists modulate postmitotic cell migration in slice cultures of embryonic rat
584 cortex. *Cereb Cortex* 10:899–909.
- 585 Ben-Ari Y (2002) Excitatory actions of GABA during development: the nature of the
586 nurture. *Nat Rev Neurosci* 3:728–739.
- 587 Ben-Ari Y, Cherubini E, Corradetti R, Gaiarsa J (1989) Giant synaptic potentials in
588 immature rat CA3 hippocampal neurones. *J Physiol* 416:303–325.
- 589 Ben-Ari Y, Gaiarsa J-L, Tyzio R, Khazipov R (2007) GABA: a pioneer transmitter that
590 excites immature neurons and generates primitive oscillations. *Physiol Rev*
591 87:1215–1284.
- 592 Ben-ari Y, Khazipov R, Leinekugel X, Caillard O, Gaiarsa J (1997) GABAA, NMDA and
593 AMPA receptors : a developmentally regulated ‘ménage à trois.’ *Trends Neurosci*
594 20:523–529.
- 595 Ben-Ari Y, Woodin MA, Sernagor E, Cancedda L, Vinay L, Rivera C, Legendre P,

- 596 Luhmann HJ, Bordey A, Wenner P, Fukuda A, van den Pol AN, Gaiarsa J-L,
597 Cherubini E (2012) Refuting the challenges of the developmental shift of polarity of
598 GABA actions: GABA more exciting than ever! *Front Cell Neurosci* 6:35.
- 599 Buchs P-A, Stoppini L, Muller D (1993) Structural modifications associated with synaptic
600 development in area CA1 of rat hippocampal organotypic cultures. *Brain Res Dev*
601 *Brain Res* 71:81–91.
- 602 Buxbaum JD, Silverman JM, Smith CJ, Greenberg D a, Kilifarski M, Reichert J, Cook
603 EH, Fang Y, Song C-Y, Vitale R (2002) Association between a GABRB3
604 polymorphism and autism. *Mol Psychiatry* 7:311–316.
- 605 Cancedda L, Fiumelli H, Chen K, Poo M (2007) Excitatory GABA action is essential for
606 morphological maturation of cortical neurons in vivo. *J Neurosci* 27:5224–5235.
- 607 Chancey JH, Adlaf EW, Sapp MC, Pugh PC, Wadiche JI, Overstreet-Wadiche LS
608 (2013) GABA depolarization is required for experience-dependent synapse
609 unsilencing in adult-born neurons. *J Neurosci* 33:6614–6622.
- 610 Chupleau C a, Larimore JL, Theibert A, Pozzo-Miller L (2009) Modulation of dendritic
611 spine development and plasticity by BDNF and vesicular trafficking: fundamental
612 roles in neurodevelopmental disorders associated with mental retardation and
613 autism. *J Neurodev Disord* 1:185–196.
- 614 Che A, Babij R, Iannone AF, Liston C, Fishell G, De Marco Garcia N V (2018) Layer I
615 Interneurons Sharpen Sensory Maps during Neonatal Development. *Neuron*
616 99:98–116.
- 617 Chen C-H, Huang C-C, Cheng M-C, Chiu Y-N, Tsai W-C, Wu Y-Y, Liu S-K, Gau SS-F
618 (2014) Genetic analysis of GABRB3 as a candidate gene of autism spectrum
619 disorders. *Mol Autism* 5:36.
- 620 De Simoni A, Griesinger CB, Edwards FA (2003) Development of rat CA1 neurones in
621 acute versus organotypic slices: role of experience in synaptic morphology and
622 activity. *J Physiol* 550:135–147.
- 623 Drakew A, Muller M, Gahwiler B, Thompson S, Frotscher M (1996) Spine Loss in
624 Experimental Epilepsy: Quantitative Light and Electron Microscopic Analysis of

- 625 Intracellularly Stained CA3 Pyramidal Cells in Hippocampal Slice Cultures.
626 Neuroscience 70:31–45.
- 627 Dzhala VI, Talos DM, Sdrulla DA, Brumback AC, Mathews GC, Benke TA, Delpire E,
628 Jensen FE, Staley KJ (2005) NKCC1 transporter facilitates seizures in the
629 developing brain. Nat Med 11:1205–1213.
- 630 El Marroun H, White T, Verhulst FC, Tiemeier H (2014) Maternal use of antidepressant
631 or anxiolytic medication during pregnancy and childhood neurodevelopmental
632 outcomes: a systematic review. Eur Child Adolesc Psychiatry 23:973–992.
- 633 Fiala JC (2005) Reconstruct : a free editor for serial section microscopy. J Microsc
634 218:52–61.
- 635 Fiala JC, Spacek J, Harris KM (2002) Dendritic Spine Pathology : Cause or
636 Consequence of Neurological Disorders ? Brain Res Rev 39:29–54.
- 637 Fiumelli H, Briner A, Puskarjov M, Blaesse P, Belem BJ, Dayer AG, Kaila K, Martin J-L,
638 Vutskits L (2012) An Ion Transport-Independent Role for the Cation-Chloride
639 Cotransporter KCC2 in Dendritic Spinogenesis In Vivo. Cereb Cortex.
- 640 Garaschuk O, Hanse E, Konnerth A (1998) Developmental profile and synaptic origin of
641 early network oscillations in the CA1 region of rat neonatal hippocampus. J Physiol
642 507 (Pt 1:219–236.
- 643 Ge S, Goh ELK, Sailor K a, Kitabatake Y, Ming G, Song H (2006) GABA regulates
644 synaptic integration of newly generated neurons in the adult brain. Nature 439:589–
645 593.
- 646 Griguoli M, Cherubini E (2017) Early Correlated Network Activity in the Hippocampus :
647 Its Putative Role in Shaping Neuronal Circuits. Front Cell Neurosci 11:1–11.
- 648 Gullledge AT, Stuart GJ (2003) Excitatory actions of GABA in the cortex. Neuron
649 37:299–309.
- 650 Haber M, Zhou L, Murai KK (2006) Cooperative Astrocyte and Dendritic Spine
651 Dynamics at Hippocampal Excitatory Synapses. 26:8881–8891.
- 652 Hanse E, Durand GM, Garaschuk O, Konnerth A (1997) Activity-dependent wiring of the

- 653 developing hippocampal neuronal circuit. *Semin Cell Dev Biol* 8:35–42.
- 654 He Q, Nomura T, Xu J, Contractor A (2014) The Developmental Switch in GABA
655 Polarity Is Delayed in Fragile X Mice. *J Neurosci* 34:446–450.
- 656 Heaulme M, Chambon JP, Leyris R, Molimard JC, Wermuth CG, Biziere K (1986)
657 Biochemical characterization of the interaction of three pyridazinyl-GABA
658 derivatives with the GABA_A receptor site. *Brain Res* 384:224–231.
- 659 Heck N, Kilb W, Reiprich P, Kubota H, Furukawa T, Fukuda A, Luhmann HJ (2007)
660 GABA-A receptors regulate neocortical neuronal migration in vitro and in vivo.
661 *Cereb Cortex* 17:138–148.
- 662 Hutsler JJ, Zhang H (2010) Increased dendritic spine densities on cortical projection
663 neurons in autism spectrum disorders. *Brain Res* 1309:83–94.
- 664 Irwin SA, Galvez R, William T (2000) Dendritic Spine Structural Anomalies in Fragile-X
665 Mental Retardation Syndrome. :1038–1044.
- 666 Irwin SA, Patel B, Idupulapati M, Harris JB, Crisostomo RA, Larsen BP, Kooy F,
667 Willems PJ, Cras P, Kozlowski PB, Swain RA, Weiler IJ, Greenough WT (2001)
668 Abnormal dendritic spine characteristics in the temporal and visual cortices of
669 patients with fragile-X syndrome: a quantitative examination. *Am J Med Genet*
670 98:161–167.
- 671 Ji Y, Lu Y, Yang F, Shen W, Tang TTT, Feng L, Duan S, Lu B (2010) Acute and gradual
672 increases in BDNF concentration elicit distinct signaling and functions in neurons.
673 *Nat Neurosci* 13:302–309.
- 674 Johnston GAR (2014) Muscimol as an Ionotropic GABA Receptor Agonist. *Neurochem*
675 *Res* 39:1942–1947.
- 676 Jourdain P, Nikonenko I, Alberi S, Muller D (2002) Remodeling of Hippocampal
677 Synaptic Networks by a Brief Anoxia – Hypoglycemia. 22:3108–3116.
- 678 Kaila K (1994) Ionic Basis of GABA_A Receptor Channel Function in the Nervous
679 System. *Prog Neurobiol* 42:489–437.
- 680 Kaufmann WE, Moser HW (2000) Dendritic Anomalies in Disorders Associated with

- 681 Mental Retardation. :981–991.
- 682 Khalilov I, Dzhala V, Ben-Ari Y, Khazipov R (1999) Dual Role of GABA in the Neonatal
683 Rat Hippocampus. *Dev Neurosci* 21:310–319.
- 684 Khalilov I, Minlebaev M, Mukhtarov M, Khazipov R (2015) Dynamic Changes from
685 Depolarizing to Hyperpolarizing GABAergic Actions during Giant Depolarizing
686 Potentials in the Neonatal Rat Hippocampus. 35:12635–12642.
- 687 Khazipov R, Leinekugel X, Khalilov I, Gaiarsa J, Ben-ari Y (1997) Synchronization of
688 GABAergic interneuronal network in CA3 subfield of neonatal rat hippocampal
689 slices. *J Physiol* 483:763–772.
- 690 Kirmse K, Hübner CA, Isbrandt D, Witte OW (2018) GABAergic Transmission during
691 Brain Development: Multiple Effects at Multiple Stages. *Neurosci* 24:36–53.
- 692 Kirmse K, Kummer M, Kovalchuk Y, Witte OW, Garaschuk O, Holthoff K (2015) GABA
693 depolarizes immature neurons and inhibits network activity in the neonatal
694 neocortex in vivo. *Nat Commun* 6.
- 695 Lacey DJ, Terplan K (1987) Abnormal Cerebral Cortical Neurons in a Child With
696 Maternal PKU Syndrome. *J Child Neurol* 2:201–204.
- 697 Lamsa KP, Palva JM, Ruusuvuori E, Kaila K, Taira T (2000) Synaptic GABA A
698 Activation Inhibits AMPA-Kainate Receptor – Mediated Bursting in the Newborn (
699 P0 – P2) Rat Hippocampus. *J Neurophysiol* 83:359–366.
- 700 Le Magueresse C, Safiulina V, Changeux J-P, Cherubini E (2006) Nicotinic modulation
701 of network and synaptic transmission in the immature hippocampus investigated
702 with genetically modified mice. *J Physiol* 576:533–546.
- 703 Leinekugel X, Tseeb V, Ben-ari Y, Bregestovski P (1995) Synaptic GABAA activation
704 induces Ca²⁺ rise in pyramidal cells and interneurons from rat neonatal
705 hippocampal slices. *J Physiol* 487:319–329.
- 706 Leonzino M, Busnelli M, Antonucci F, Verderio C, Mazzanti M, Chini B, Leonzino M,
707 Busnelli M, Antonucci F, Verderio C, Mazzanti M, Chini B (2016) The Timing of the
708 Excitatory-to-Inhibitory GABA Switch Is Regulated by the Oxytocin Receptor Report
709 The Timing of the Excitatory-to-Inhibitory GABA Switch Is Regulated by the

- 710 Oxytocin Receptor via KCC2. :96–103.
- 711 Li H, Khirug S, Cai C, Ludwig A, Blaesse P, Kolikova J, Afzalov R, Coleman SK, Lauri
712 S, Airaksinen MS, Keinänen K, Khiroug L, Saarma M, Kaila K, Rivera C (2007)
713 KCC2 interacts with the dendritic cytoskeleton to promote spine development.
714 *Neuron* 56:1019–1033.
- 715 Liu X, Wang Q, Haydar TF, Bordey A (2005) Nonsynaptic GABA signaling in postnatal
716 subventricular zone controls proliferation of GFAP-expressing progenitors. *Nat*
717 *Neurosci* 8:1179–1187.
- 718 Megias M, Emri Z, Gulyas A, Freund T (2001) Total number and distribution of inhibitory
719 and excitatory synapses on hippocampal CA1 pyramidal cells. *Neuroscience*
720 102:527–540.
- 721 Menold MM, Shao Y, Wolpert CM, Donnelly SL, Raiford KL, Martin ER, Ravan S a,
722 Abramson RK, Wright HH, DeLong GR, Cuccaro ML, Pericak-Vance M a, Gilbert JR
723 (2001) Association analysis of chromosome 15 gabaa receptor subunit genes in
724 autistic disorder. *J Neurogenet* 15:245–259.
- 725 Mohajerani MH, Cherubini E (2005) Spontaneous recurrent network activity in
726 organotypic rat hippocampal slices. *Eur J Neurosci* 22:107–118.
- 727 Mortensen M, Ebert B, Wafford K, Smart TG (2010) Distinct activities of GABA agonists
728 at synaptic- and extrasynaptic-type GABAA receptors. *J Physiol* 588:1251–1268.
- 729 Muller D, Buchs P-A, Stoppini L (1993) Time course of synaptic development in
730 hippocampal organotypic cultures. *Brain Res Dev Brain Res* 71:93–100.
- 731 Oh WC, Lutz S, Castillo PE, Kwon HB (2016) De novo synaptogenesis induced by
732 GABA in the developing mouse cortex. *Science* (80-) 353.
- 733 Owens DF, Kriegstein AR (2002) Is there more to GABA than synaptic inhibition? *Nat*
734 *Rev Neurosci* 3:715–727.
- 735 Park H, Poo MM (2013) Neurotrophin regulation of neural circuit development and
736 function. *Nat Rev Neurosci* 14:7–23.
- 737 Pérez-Gómez A, Tasker RA (2013) Transient domoic acid excitotoxicity increases

- 738 BDNF expression and activates both MEK- and PKA-dependent neurogenesis in
739 organotypic hippocampal slices. *BMC Neurosci* 14:72.
- 740 Puskarjov M, Ahmad F, Khirug S, Sivakumaran S, Kaila K, Blaesse P (2014) BDNF is
741 required for seizure-induced but not developmental up-regulation of KCC2 in the
742 neonatal hippocampus. *Neuropharmacology* 88:1–7.
- 743 Puskarjov M, Fiumelli H, Briner A, Bodogan T, Demeter K, Laco C, Mavrovic M,
744 Blaesse P, Kaila K, Vutskits L (2017) K-Cl Cotransporter 2-mediated Cl⁻ extrusion
745 determine developmental stage-dependent impact of propofol mediated anesthesia
746 on dendritic spines. *Anesthesiology* 126:1–13.
- 747 Rivera C, Voipio J, Payne JA (1999) The K⁺/Cl⁻ co-transporter KCC2 renders GABA
748 hyperpolarizing during neuronal maturation. *Nature* 397:251–255.
- 749 Rodriguez A, Ehlenberger DB, Dickstein DL, Hof PR, Wearne SL (2008) Automated
750 three-dimensional detection and shape classification of dendritic spines from
751 fluorescence microscopy images. *PLoS One* 3.
- 752 Sedmak G, Jovanov-Milošević N, Puskarjov M, Ulamec M, Krušlin B, Kaila K, Judaš M
753 (2015) Developmental Expression Patterns of KCC2 and Functionally Associated
754 Molecules in the Human Brain. *Cereb Cortex*:1–16.
- 755 Sokal DM, Mason R, Parker TL (2000) Multi-neuronal recordings reveal a differential
756 effect of thapsigargin on bicuculline- or gabazine-induced epileptiform excitability in
757 rat hippocampal neuronal networks. *Neuropharmacology* 39:2408–2417.
- 758 Staley KJ, Mody I (1992) Shunting of excitatory input to dentate gyrus granule cells by a
759 depolarizing GABAA receptor-mediated postsynaptic conductance. *J Neurophysiol*
760 68:197–212.
- 761 Staley KJ, Proctor WR (1999) Modulation of mammalian dendritic GABAA receptor
762 function by the kinetics of Cl⁻ and HCO₃⁻ transport. *J Physiol* 519:693–712.
- 763 Swann JW, Brady RJ, Martin DL (1989) Postnatal development of GABA-mediated
764 synaptic inhibition in rat hippocampus. *Neuroscience* 28:551–561.
- 765 Tyler WJ, Pozzo-Miller L (2003) Miniature synaptic transmission and BDNF modulate
766 dendritic spine growth and form in rat CA1 neurones. *J Physiol* 553:497–509.

- 767 Tyzio R, Nardou R, Ferrari DC, Tsintsadze T, Shahrokhi A, Eftekhari S, Khalilov I,
768 Tsintsadze V, Brouchoud C, Chazal G, Lemonnier E, Lozovaya N, Burnashev N,
769 Ben-Ari Y (2014) Oxytocin-Mediated GABA Inhibition During Delivery Attenuates
770 Autism Pathogenesis in Rodent Offspring. *Science* (80-) 343:675–680.
- 771 Valeeva G, Tressard T, Mukhtarov M, Baude A, Khazipov R (2016) An Optogenetic
772 Approach for Investigation of Excitatory and Inhibitory Network GABA Actions in
773 Mice Expressing Channelrhodopsin-2 in GABAergic Neurons. *J Neurosci* 36:5961–
774 5973.
- 775 Vanhatalo S, Palva JM, Andersson S, Rivera C, Voipio J, Kaila K (2005) Slow
776 endogenous activity transients and developmental expression of K⁺-Cl⁻
777 cotransporter 2 in the immature human cortex. *Eur J Neurosci* 22:2799–2804.
- 778 Vicario-Abejón C, Collin C, McKay RD, Segal M (1998) Neurotrophins induce formation
779 of functional excitatory and inhibitory synapses between cultured hippocampal
780 neurons. *J Neurosci* 18:7256–7271.
- 781 Vicario-Abejón C, Owens D, McKay R, Segal M (2002) Role of neurotrophins in central
782 synapse formation and stabilization. *Nat Rev Neurosci* 3:965–974.
- 783 Wang DD, Kriegstein AR (2008) GABA regulates excitatory synapse formation in the
784 neocortex via NMDA receptor activation. *J Neurosci* 28:5547–5558.
- 785 Wang DD, Kriegstein AR (2009) Defining the role of GABA in cortical development. *J*
786 *Physiol* 587:1873–1879.
- 787 Wang DD, Kriegstein AR (2011) Blocking early GABA depolarization with bumetanide
788 results in permanent alterations in cortical circuits and sensorimotor gating deficits.
789 *Cereb Cortex* 21:574–587.
- 790 Wells JE, Porter JT, Agmon A, Virginia W (2000) GABAergic Inhibition Suppresses
791 Paroxysmal Network Activity in the Neonatal Rodent Hippocampus and Neocortex.
792 *J Neurosci* 20:8822–8830.
- 793 Yamada J, Okabe A, Toyoda H, Kilb W, Luhmann HJ, Fukuda A (2004) Cl⁻ uptake
794 promoting depolarizing GABA actions in immature rat neocortical neurones is
795 mediated by NKCC1. *J Physiol* 557:829–841.

796 Zeng L, Xu L, Rensing NR, Sinatra PM, Rothman SM, Wong M (2007) Kainate Seizures
797 Cause Acute Dendritic Injury and Actin Depolymerization In Vivo. *J Neurosci*
798 27:11604–11613.

799 Zha X-M, Green SH, Dailey ME (2005) Regulation of hippocampal synapse remodeling
800 by epileptiform activity. *Mol Cell Neurosci* 29:494–506.

801

802

803

804

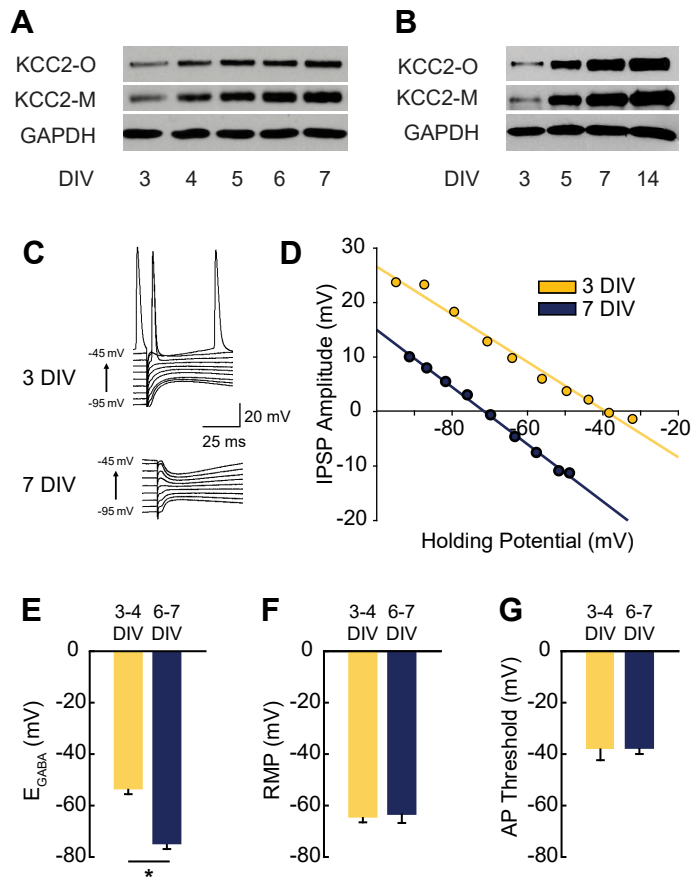


Figure 1

Figure 1. GABA reversal potential (E_{GABA}) shifts from depolarizing to hyperpolarizing between 3 and 7 DIV. *A-B*, High (A) and low (B) temporal resolution western blots showing increasing expression of KCC2 monomers (KCC2-M) and oligomers (KCC2-O). *C-D*, Representative traces and representative IV curves from GABAergic responses at 3DIV and 7DIV. *E*, E_{GABA} summary plots (3/4 DIV: -53.3 ± 6.1 mV, $n=5$; 6/7 DIV: -74.7 ± 6.4 mV, $n=5$, $p=0.04$). *F*, Resting membrane potential summary plots (3/4 DIV: -64.5 ± 2.3 mV, $n=5$; 6/7 DIV: -63.4 ± 3.8 mV, $n=5$). *G*, Action potential threshold summary plot (3/4 DIV: -38.2 ± 4.2 mV, $n=5$; 6/7 DIV: -37.7 ± 2.3 mV, $n=5$).

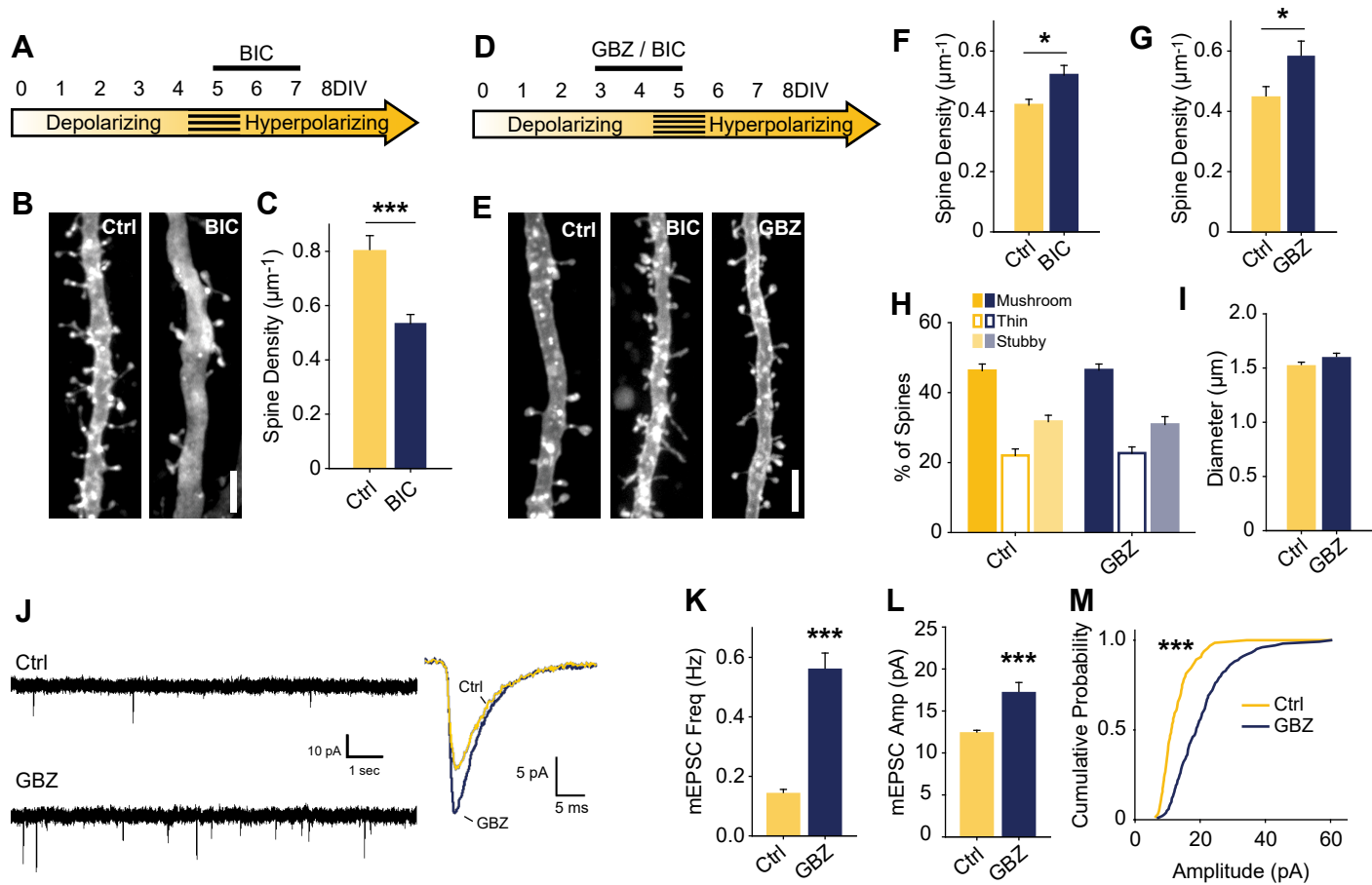


Figure 2

Figure 2. Blocking depolarizing GABA_A transmission increases excitatory synapse number. **A**, Time course of bicuculline (BIC) treatment for B-C. **B-C**, Spine density after 5-7 DIV BIC treatment (Control 0.80 ± 0.06 spines/um, $n=36$, BIC 0.53 ± 0.03 , $n=50$; $N=3$; $p < 0.001$, Mann-Whitney). **D**, Time course of pharmacological treatments for E-M. **E-G**, Spine density after 3-5 DIV GBZ (G: Control 0.44 ± 0.12 spines/um, $n=145$, GBZ 0.58 ± 0.17 , $n=77$; $N=11$; $p=0.04$) and BIC treatment (F: Control 0.42 ± 0.02 spines/um, $n=55$, BIC 0.52 ± 0.03 spines/um, $n=41$; $N=9$; $P=0.027$, Mann-Whitney). **H,I**, 3D spine morphology and dendrite diameter after GBZ. **J**, Representative traces of mEPSCs. **K**, mEPSC frequency summary plot (Control 0.14 ± 0.02 Hz, GBZ 0.56 ± 0.06 Hz, $p < 0.001$, Mann-Whitney). **L**, mEPSC amplitude summary plot (Control 12.32 ± 0.37 pA, $n=8$, GBZ 17.12 ± 1.27 pA, $n=10$, $p < 0.001$, Mann-Whitney). **M**, Cumulative distributions of amplitudes ($p < 0.0001$, Kolmogorov-Smirnov test). Scale bars $3 \mu\text{m}$.

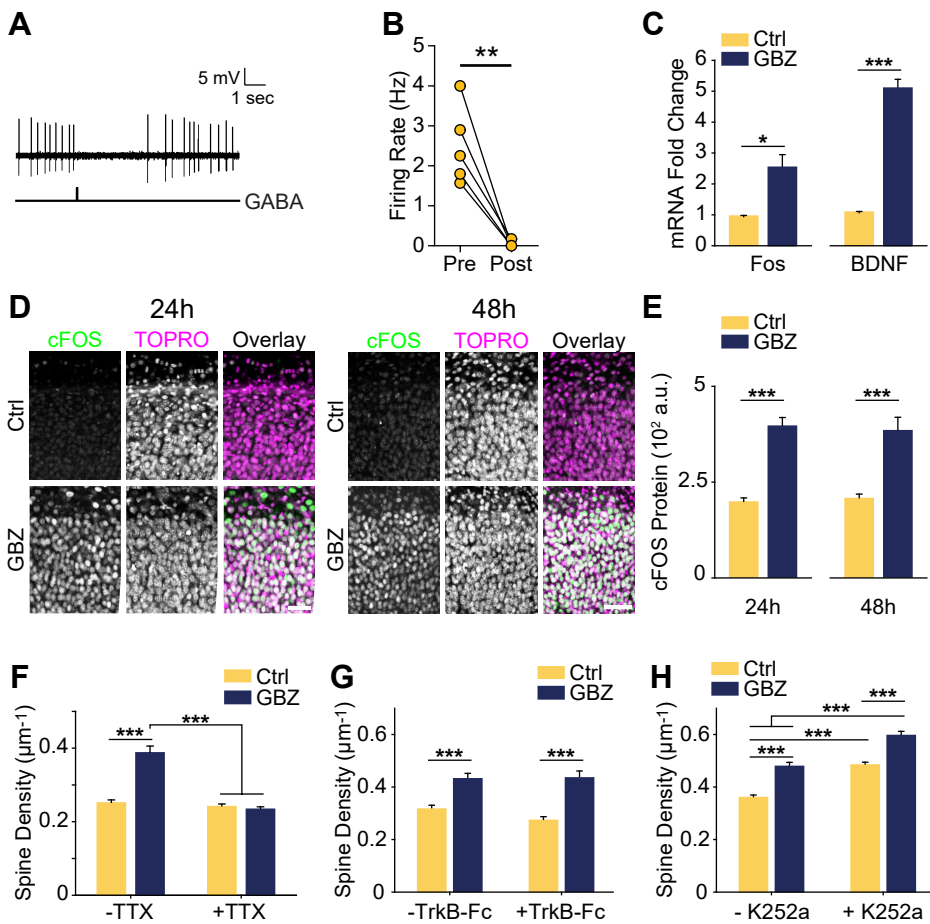


Figure 3

Figure 3. Increase in spine density following blockade of depolarizing/inhibitory GABA_A transmission is activity-dependent but does not rely on BDNF signalling. .

A, Sample trace of spontaneous activity inhibited by puffing on GABA. The line trace below indicates time of GABA puff. **B**, Summary plots of spontaneous activity pre- and post-GABA puff. **C**, BDNF and Fos transcript levels following GBZ from 3-5DIV (BDNF: Ctrl 1.07 ± 0.04 , GBZ 5.08 ± 0.3 , N=3, $p < 0.001$; Fos: Ctrl 0.94 ± 0.04 , GBZ 2.52 ± 0.4 , N=3, $p = 0.02$). **D**, Fos immunofluorescence 24 and 48 hours after GBZ treatment at 3DIV. Images depict the dividing line between stratum oriens (upper portion of panels) and stratum pyramidale (lower portion of panels) in area CA1. TOPRO-3-Iodide was used to visualize nuclei. **E**, Quantification of Fos immunofluorescence following 24h (Ctrl 196.5 ± 12.2 au, n=10, GBZ 394.4 ± 24.0 au, n=11, $p < 0.001$) and 48h (Ctrl 205.6 ± 12.1 au, n=10, GBZ 382.7 ± 36.3 au, n=10, $p < 0.001$, Mann-Whitney) of GBZ treatment which started at 3DIV. **F**, Quantification of spine density following GBZ and/or TTX treatment beginning at 3DIV (Ctrl $0.25 \pm 0.01 \mu\text{m}^{-1}$, n= 196, GBZ $0.39 \pm 0.01 \mu\text{m}^{-1}$, n=110, TTX $0.24 \pm 0.01 \mu\text{m}^{-1}$, n= 166, GBZ+TTX $0.23 \pm 0.01 \mu\text{m}^{-1}$, n=154; N=5). Two-way ANOVA indicates a significant interaction between GBZ and TTX conditions, $p < 0.001$. Significant differences between GBZ and all other conditions, $p < 0.001$, Tukey post test. **G**, Quantification of spine density following GBZ and/or TrkB-Fc treatment (Ctrl 0.31 ± 0.02 , n=86, GBZ 0.42 ± 0.02 , n=68, TrkB-Fc 0.27 ± 0.02 , n=96, TrkB-Fc+GBZ 0.43 ± 0.02 , n=61; N=3; 2 Way ANOVA, no interaction, Tukey post test). **H**, Quantification of spine density following GBZ and/or K252a treatment (Ctrl 0.35 ± 0.01 , n=198, GBZ 0.49 ± 0.03 , n=144, K252a 0.47 ± 0.02 , n= 216, K252a+GBZ 0.58 ± 0.04 , n=185; all significant differences < 0.001 , 2 Way ANOVA, no interaction, Tukey post test).

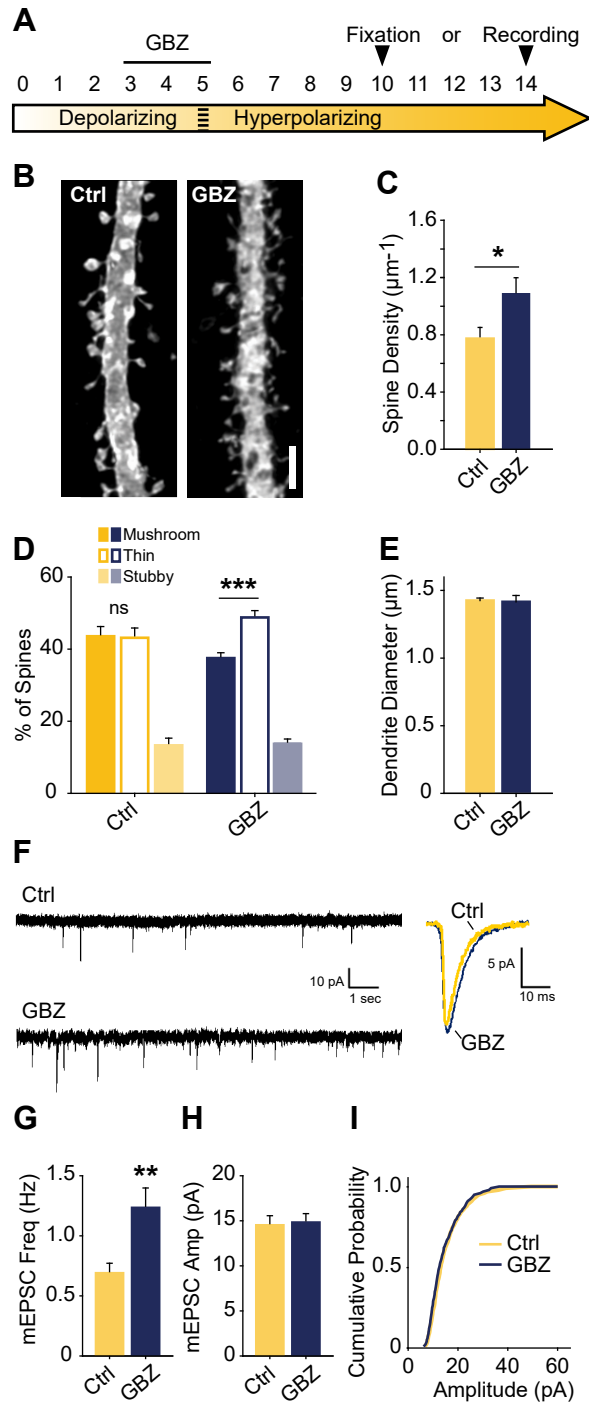
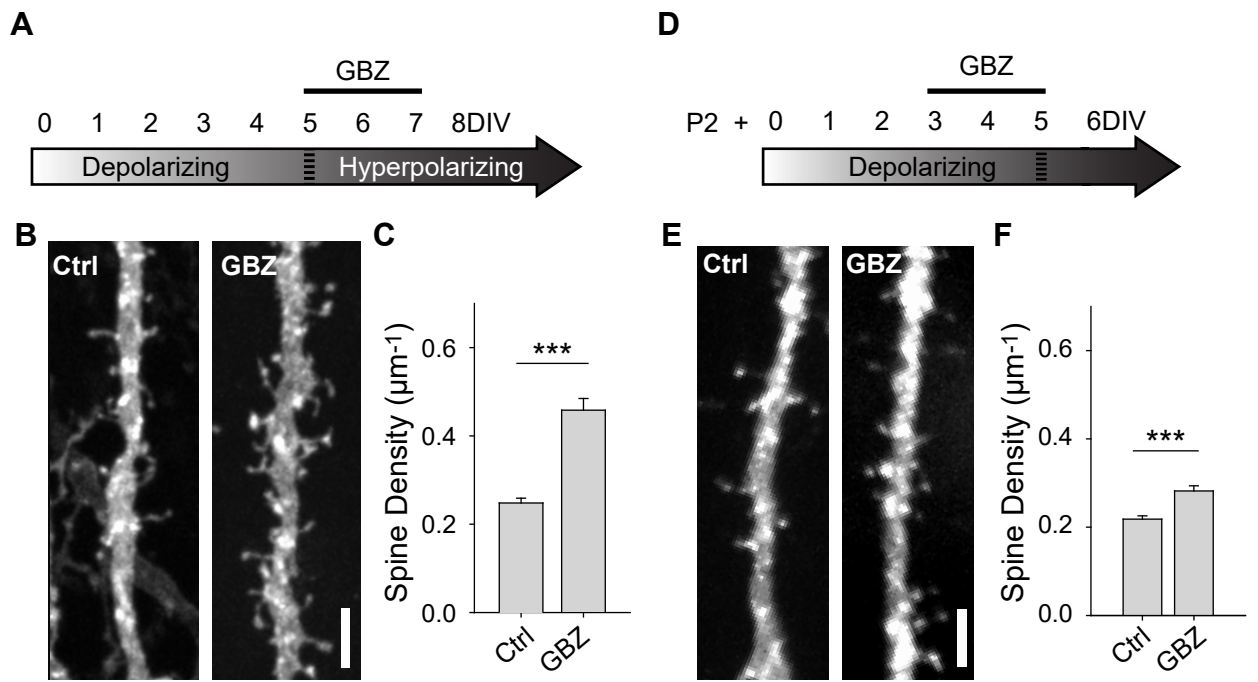


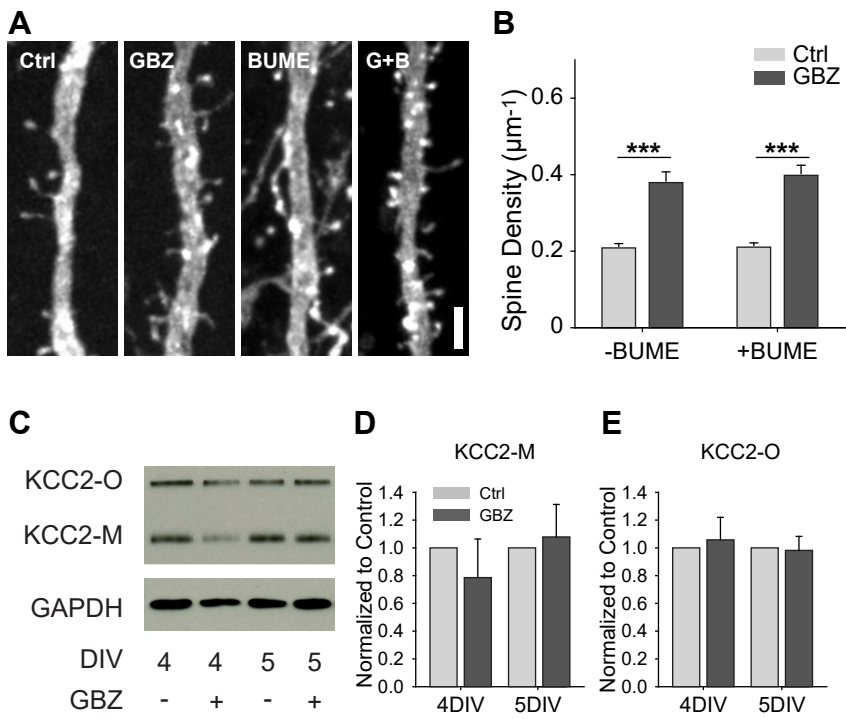
Figure 4

Figure 4. Transient blockade of depolarizing GABA_A transmission causes a lasting increase in excitatory synapses and alters spine morphology. **A**, Schematic time course of GBZ treatment and experimental endpoints. **B,C**, Spine density after 3-5 DIV GBZ treatment and 5 days of recovery (Control 0.78 ± 0.08 spines/ μm , $n=127$; GBZ washout 1.07 ± 0.07 spines/ μm , $n=112$; $N=6$; $p=0.024$). **D**, 3D spine morphology after 5 days of recovery ($***p < 0.001$, critical level 0.05, Two Way ANOVA with Holm Sidak Post Test). **E**, Dendrite diameter after recovery ($p=0.86$). **F**, Representative mEPSC traces from slices after 8-9 days recovery. **G**, mEPSC frequency summary plot (Control: 0.70 ± 0.08 Hz, $n=10$ GBZ: 1.23 ± 0.17 Hz, $n=10$, $p=0.009$). **H**, mEPSC amplitude summary plot (Control: 14.50 ± 1.07 pA, $n=10$, GBZ: 14.80 ± 1.00 pA, $n=10$, $p=0.84$). **I**, Cumulative mEPSC distributions ($p=0.58$, Kolmogorov-Smirnov test). Scale bar $3\mu\text{m}$.



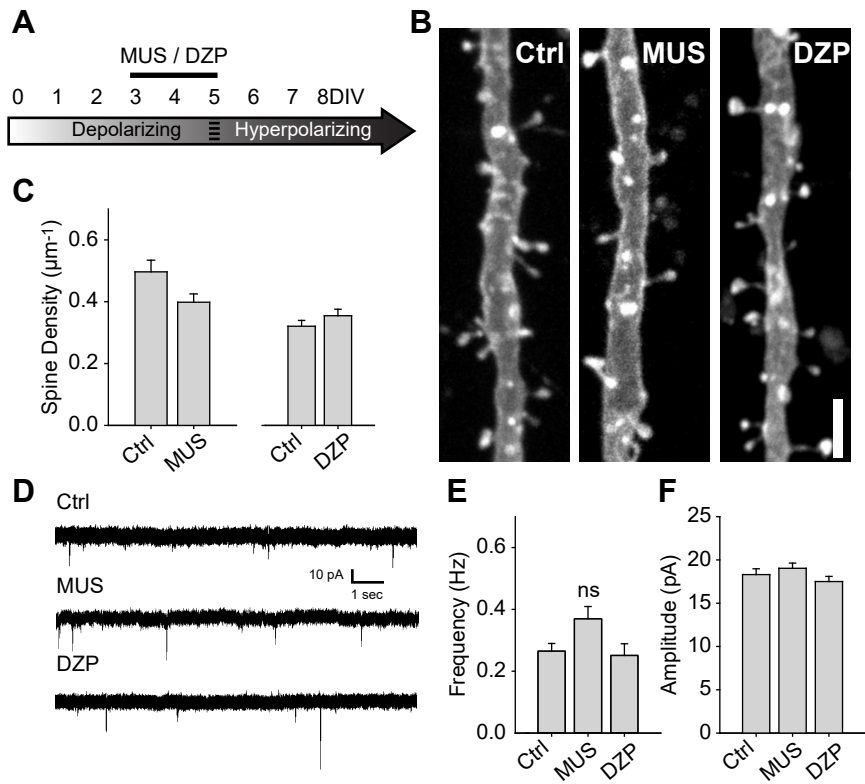
Supporting Figure 1

S1 Fig. GBZ-induced increase in spines is preserved in absence of antibiotics and in slices cultured from P2 mice. **A**, Time course of antibiotic-free GBZ treatment. **B,C**, Exemplary images and quantification of the spine enhancing effect of GBZ on slices cultures in antibiotic-free culture medium (Ctrl $0.248 \pm 0.0109 \mu\text{m}^{-1}$, $n=198$, GBZ $0.458 \pm 0.0264 \mu\text{m}^{-1}$, $n=70$; $N=4$; $p < 0.001$, Mann-Whitney). **D**, Time course of treatment of slices prepared from P2 pups. **E,F**, Exemplary images and quantification of spine enhancing effect of GBZ when applied to slices from P2 pups (Ctrl $0.22 \pm 0.008 \mu\text{m}^{-1}$, $n=217$, GBZ $0.28 \pm 0.01 \text{ spines}/\mu\text{m}^{-1}$, $n=156$; $N=3$; $p < 0.001$, Mann Whitney).



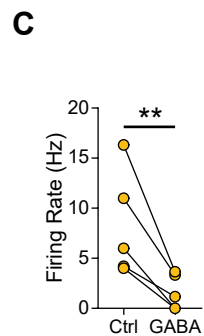
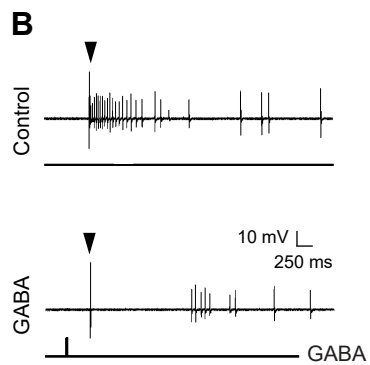
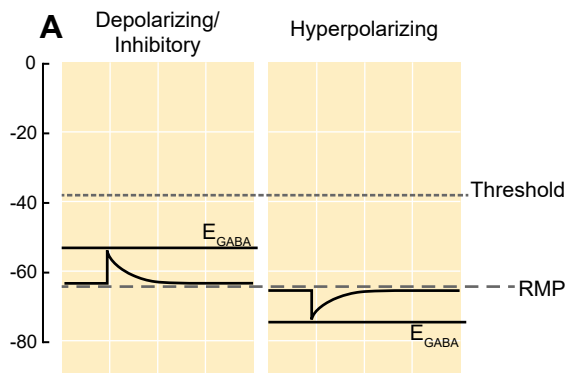
Supporting Figure 2

S2 Fig. GBZ-induced increase in spines is not reproduced by bumetanide and is not associated with changes in KCC2 expression. A,B, Bumetanide does not increase spine density above control levels, (B, Control $0.21 \pm 0.01 \text{ } \mu\text{m}^{-1}$, $n=102$; GBZ $0.38 \pm 0.02 \text{ } \mu\text{m}^{-1}$, $n=47$; BUME $0.21 \pm 0.02 \text{ } \mu\text{m}^{-1}$, $n=88$; BUME+GBZ $0.40 \pm 0.02 \text{ } \mu\text{m}^{-1}$, $n=53$; $N=3$; Two-way ANOVA indicated no significant interaction between GBZ and BUME treatment ($p=0.633$). Tukey HSD post test indicates significant differences between Ctrl and GBZ in the absence of BUME ($p<0.001$) and in the presence of BUME ($p<0.001$)). **C-E,** Western blot (C) showing no changes in monomeric (D) or oligomeric (E) KCC2 expression following GBZ from 3-4DIV ($p=0.52$ and 0.77 , respectively, One Sample t-Test, $n=3$) and 3-5 DIV ($p=0.76$ and 0.87 , respectively, One Sample t-Test, $n=3$). Scale bar $3\mu\text{m}$.



Supporting Figure 3

S3 Fig. Driving depolarizing GABA_A transmission does not decrease glutamatergic synapse numbers. **A**, Time course of MUS and DZP treatment. **B,C**, Spine density after 3-5 DIV MUS treatment (Ctrl 0.50 ± 0.04 , n=32; MUS 0.40 ± 0.03 , n=39; N=7; p = 0.07) and DZP treatment (Ctrl 0.321 ± 0.02 , n=116; DZP 0.36 ± 0.02 , n=88; N=6; p = 0.11, Mann-Whitney). **D**, Representative traces of mEPSCs following 3-5DIV treatment with MUS or DZP. **E**, mEPSC frequency summary plot (Ctrl: 0.27 ± 0.02 Hz, n=9; MUS: 0.37 ± 0.04 Hz, n=8; DZP: 0.25 ± 0.04 Hz, n=8; One way ANOVA p=0.046; Ctrl vs MUS, p=0.09; Ctrl vs DZP, p=0.9). **F**, mEPSC amplitude summary plot (Ctrl: 18.3 ± 0.7 pA, n=9; MUS: 19.0 ± 0.6 pA, n=8; DZP: 17.5 ± 0.6 pA, n=8; One Way ANOVA, p=0.263)



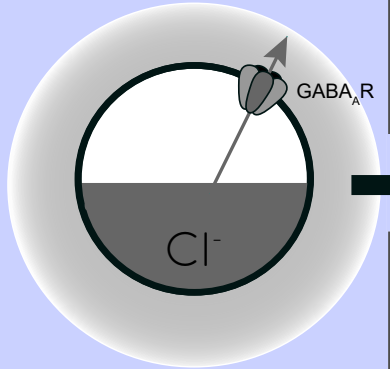
Supporting Figure 4

S4 Fig. Shunting GABA transmission inhibits electrically evoked firing in CA1 neurons at 3DIV. **A**, Schematic demonstrating the likely shunting and hence inhibitory nature of GABA_A transmission due to the relative values of AP Threshold > E_{GABA} > RMP. The scale in A aligns with that of *Fig 1 E, F* and *G* such that the threshold, RMP and E_{GABA} values are represented accurately relative to each other. **B**, Sample traces from the same cell demonstrating that activity could be evoked electrically (Control) and that puffed GABA inhibited electrically evoked activity (GABA). The arrow above the traces denotes the timing of electrical stimulation. **C**, Summary plots of electrically evoked activity in the absence and presence of puffed GABA.

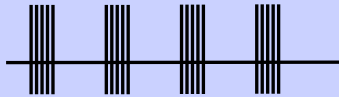
Model 1

A

Depolarizing GABA



Basal Activity



GABA Blockade

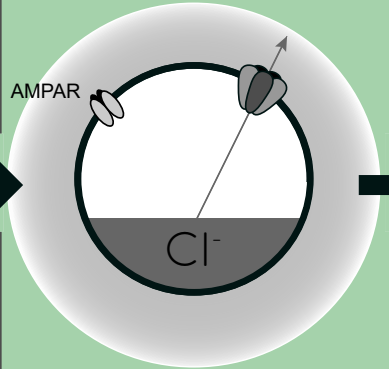


Disrupted synapse formation and maturation

Model 2

B

Depolarizing/Inhibitory GABA



Basal Activity



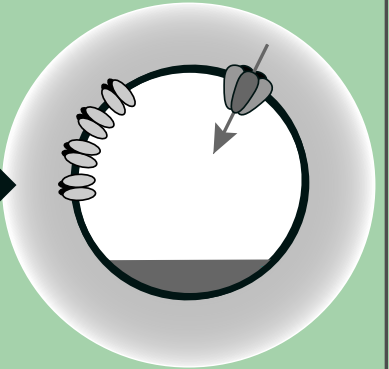
GABA Blockade



Activity-dependent increase in synapse formation and maturation

C

Hyperpolarizing GABA



Basal Activity



GABA Blockade



Synapse loss due to overexcitation

Supporting Figure 5

S5 Fig. A model of the possible roles of GABA_A transmission in glutamatergic synapse formation as chloride homeostasis matures. A, Work performed in acute slices suggests that depolarizing GABA_A transmission provides the initial excitatory drive required for activity- and calcium-dependent formation and maturation of glutamatergic synapses. Blocking GABA_A transmission at this stage eliminated GDPs. For the sake of simplicity we have depicted that GABA_A blockade would eliminate GDPs and silence network activity at this stage, however it should be noted that in acute slices, blocking GABA_A transmission at this point has been shown to decrease circuit activity in immature acute hippocampal slices as depicted (Ben-Ari et al., 1989; Garaschuk et al., 1998; Mohajerani and Cherubini, 2005), but has also been shown to induce interictal discharges (Khazipov et al., 1997; Khalilov et al., 1999; Lamsa et al., 2000) or paroxysmal activity (Wells et al., 2000). These latter effects may be due to an overarching inhibitory role for GABA during development. **B,** Our work suggests a possible transition state wherein blocking GABA_A transmission alleviates a depolarizing but inhibitory restraint on circuit activity, allowing for activity dependant formation of glutamatergic synapses. Such a transition state would likely rely on a still underdeveloped glutamatergic system that is not yet capable of pathological levels of overexcitation. Importantly, recent *in vivo* work suggests that GABA may be inhibit circuit activity throughout postnatal development, indicating that blocking GABA_A transmission might enhance glutamatergic synapse formation from birth until GABA becomes fully hyperpolarizing. (Although the basal activity here is depicted as uncoordinated to clearly differentiate A from B, the activity pattern in this transition state, as well as in C, may very well be composed of ENOs.) **C,** When E_{Cl} and the glutamatergic system are mature, blocking hyperpolarizing GABA_A transmission causes overexcitation and loss of glutamatergic synapses.